Soft Matter

Order–order transitions in poly(N-octadecyl acrylamide-co-hydroxyethyl acrylamide) statistical copolymer films

Journal:	*Soft Matter*
Manuscript ID	SM-ART-03-2023-000265.R1
Article Type:	Paper
Date Submitted by the Author:	21-Mar-2023
Complete List of Authors:	Kikuchi, Mao; Yamagata University, Faculty of Science Saito, Nozomi; Yamagata University, Faculty of Science Ohke, Mizuki; Yamagata University, Graduate School of Science and Engineering Nishitsuji, Shotaro; Yamagata University, Graduate School of Science and Engineering Nagano, Shusaku; Rikkyo University, Department of Chemistry, College of Science Matsui, Jun; Yamagata University, Faculty of Science

Order–order transitions in poly(*N*-octadecyl acrylamide-co-hydroxyethyl acrylamide) statistical copolymer films

Mao Kikuchi[†], Nozomi Saito[‡], Mizuki, Ohke[†], Shusaku Nagano[§], Shotaro Nishitsuji[⊥], and Jun Matsui[‡]

[†]Graduate School of Science and Engineering, [‡]Faculty of Science, Yamagata University, 1-4-12 Kojirakawa-machi, Yamagata 990-8560, Japan

[§] College of Science, Rikkyo University, 3-34-1 Nishi-Ikebukuro, Toshima-ku, Tokyo 171-8501, Japan

[⊥]Graduate School of Organic Materials Science, Yamagata University, 4-3-16, Jonan, Yonezawa, 992-8510, Japan

ABSTRACT: This study demonstrates that a simple statistical copolymer can form self-assembled lamellae, whose structures depend on both the comonomer composition and the annealing temperature. Statistical copolymers of octadecyl acrylamide and hydroxyethyl acrylamide [p(ODA/HEAm)] were prepared via free-radical copolymerization, and their thermal properties were studied by differential scanning calorimetry. Thin films of p(ODA/HEAm) were prepared via spin-coating, and their structures were analyzed using X-ray diffraction. It was found that copolymers with HEAm contents between 28 and 50% formed self-assembled lamellae upon annealing at a temperature ~10 °C above the glass-transition temperature. The self-assembled form was found to possess a "side-chain-mixed" lamellar structure, in which the ODA and HEAm side chains are oriented perpendicular to the lamellar plane composed of the polymer main chain. Interestingly, a copolymer with a HEAm content between 36 and 50% transformed from the side-chain-mixed lamellar structure to generate a "side-chain-segregated" lamellar structure upon annealing at a significantly higher temperature (~50 °C above *T*g). In this structure, the ODA and HEAm side chains were found to be oriented in opposite directions but perpendicular to the lamellar plane. The packing of the side chains in the lamellar structures was studied using Fourier-transform infrared spectroscopy. It was concluded that the structures of the self-assembled lamellae are determined by the strain forces generated during self-assembly, and by the segregation forces existing between the comonomers.

INTRODUCTION

Diblock copolymers consist of two homopolymers tethered together, wherein these homopolymers possess different chemical properties. It is well known that microphase separation between the individual blocks of block copolymers can facilitate the formation of unique self-assembled structures, such as lamellae, cylinders, and spheres. In addition, it has been revealed both experimentally and theoretically that the structure of the resulting self-assembled species depends on the relationship between $\chi \times N$ and the variable ϕ_1, wherein χ is the Flory–Huggins segmental interaction parameter, N is the degree of polymerization, and ϕ_1 is the volume fraction of a single block.[1-4] The generated structures are determined primarily by ϕ_1, and they have been reported to change from random spheres to cylinders and later to lamellae as ϕ_1 increases from 0 to 50%.[4] The self-assembled structures can also be converted from one structure to another, such as from cylinders to lamellae, upon variation in the annealing temperature; this process is known as an order–order transition.[5-7]

Compared to diblock copolymers, statistical (or random) copolymers can be prepared relatively easily by mixing two monomers in solution and carrying out a copolymerization reaction. Since statistical copolymers combine the properties of their constituent monomers, they have been applied in various fields, ranging from packaging and electronic devices to surface modification.[8] For example, photo-electro functional thin films can be prepared using copolymers of dyes and/or organometallic complexes using film-forming monomers such as styrene and methyl methacrylate.[9, 10] In addition, random copolymers composed of hydrophilic and hydrophobic monomers act as adhesion layers for two immiscible polymer films,[11] although they can also act as neutralization layers to control the alignment of the self-assembled structures of diblock copolymers.[12] Moreover, amphiphilic random copolymers can self-assemble to form micelles and vesicles in water, generating structures that are similar to those

observed for amphiphilic molecules.[13] However, to date, little research has been carried out on the self-assembled structures present in the solid state.

It has been reported that segregation between hydrophobic side chains and a hydrophilic main chain occurs in comb-shaped homopolymers and statistical copolymers in the solid state.[14-17] For example, Beiner et al., reported that the alkyl side chains present in comb-shape polymers can aggregate to form alkyl nanodomains due to segregation (i.e., nanophase separation).[14, 18, 19] They also reported that the alkyl nanodomains exhibit a thermal relaxation process defined as a polyethylene-like glass transition, which is decoupled with the conventional glass transition process.[15, 16] Furthermore, a thermal transition has been observed when the side chain lengths are longer than eight alkyl carbon units, and this results in crystallization/melting of the alkyl side chains (T_M).[20, 21] However, the segregation forces are low and long-range ordered structure formation is limited to side chain and/or main chain (liquid)crystalline polymers.[22-27] In contrast, our group previously reported that amorphous homo and statistical copolymers of poly(alkyl acrylamide) and poly(alkyl acrylate) form highly oriented lamellar structures upon annealing above their glass transition temperatures (T_g) under humid conditions.[28-33] The driving force for the formation of this lamellar structure is considered to be an increase in the nanophase separation force upon the adsorption of water at the hydrophilic amide or acrylate groups.[31-33] Furthermore, a statistical copolymer of dodecyl acrylamide and hydrophilic vinyl phosphoric acid was reported to form a self-assembled lamellar structure upon conventional thermal annealing above its T_g due to phase separation between the hydrophilic dodecyl side chain and the hydrophilic phosphoric acid groups.[34] These previous studies indicate that even in homo and statistical copolymers, self-assembled structures can be formed via segregation of the main and side chains and/or comonomers.

Recently, Ouchi et al. reported that an alternate copolymer of *N*-octadecyl acrylamide (ODA) and hydroxyethyl acrylamide (HEAm) self-assembled to form a lamellar structure, whereas the

same copolymer with a random sequence remained amorphous.[35] However, based on our reports on the formation of lamellae from alkyl acrylamide homo(co)polymers,[30-34] we considered that thin films constructed from p(ODA/HEAm) statistical copolymers can form lamellar structures based on the segregation between the ODA and HEAm components.

This study reports the synthesis of statistical copolymers of ODA and HEAm with different compositions and the structures of their self-assembled thin films were characterized. In particular, the "side-chain-mixed" and "side-chain-segregated" lamellar structures were investigated. The "side-chain-mixed" lamellar structure exhibits alkyl side chains oriented perpendicular to the main chain and which are present on both side of the main chain. [27, 30, 34, 36] In this structure, each lamellar sheet is stacked by the association of its alkyl side chains (tail-to-tail). On the other hand, in the "side-chain-segregated" lamellar structure, the alkyl side chain is oriented in a single direction with respect to the main chain while the hydrophilic side chain is oriented in the other direction. The side-chain-segregated lamellar sheets are stacked so that the hydrophilic side chains (head-to-head) and the hydrophobic side chains (tail-to-tail) self-associate.[23, 27, 37] Although it has been reported that homopolymers and statistical copolymers form lamellar structures via nanophase separation, no previous reports have described the fabrication of these two lamellar structures separately. Analogous to block copolymers, it is expected that the generated structure may depend on the comonomer content and the annealing temperature, and so the effects of these factors are evaluated for the prepared statistical copolymers, wherein the structures of the comonomer films are determined by X-ray diffraction (XRD). In addition, the effect of the HEAm content and annealing temperature on the lamellar structure is discussed based on the strain in the polymer chains and the miscibility of the comonomers.

MATERIALS AND METHODS

Materials

Octadecyl amine (>85%, Tokyo Chemical Industry Co., Ltd., Japan), acryloyl chloride (>98.0%, Tokyo Chemical Industry Co., Ltd., Japan), 2-hydroxyethyl acrylamide (HEAm, >98.0% Tokyo Chemical Industry Co., Ltd., Japan), triethylamine (>99.0%, Tokyo Chemical Industry Co., Ltd., Japan), trichloro(octyl)silane (97%, Sigma-Aldrich Co. LLC, Japan), acetone (guaranteed reagent grade, Nacalai Tesque Inc., Japan), isopropyl alcohol (guaranteed reagent grade, Nacalai Tesque Inc., Japan), chloroform (guaranteed reagent grade, Kanto Chemical, Japan), toluene (super dehydrated grade, FUJIFILM Wako Pure Chemical Corporation, Japan), DMF (super dehydrated grade, FUJIFILM Wako Pure Chemical Corporation, Japan), and acetonitrile (guaranteed reagent grade, Nacalai Tesque Inc., Japan) were used as received. 2,2′ -Azobisisobutyronitrile (>98.0%, AIBN, FUJIFILM Wako Pure Chemical Corporation, Japan) was recrystallized from ethanol.

Synthesis

ODA was synthesized following a previously reported method.[35] More specifically, octadecyl amine (3.60 g) was dissolved in chloroform (60 mL) and stirred at 0 °C. Triethylamine (2.00 mL) was then added to this solution, followed by dropwise addition of acryloyl chloride (1.17 mL). After the addition of acryloyl chloride, the reaction mixture was stirred at 20 °C for 4 h prior to the addition of methanol (5 mL). Subsequently, the majority of solvent was evaporated under reduced pressure, and THF (120 mL) was added. The resulting precipitate was filtered, and the filtrate was evaporated under reduced pressure to precipitate a white solid. The white solid product was dissolved in methanol (300 mL) and stored in a refrigerator for 1 day to promote the recrystallization of ODA. The compound was characterized using ^{1}H NMR spectroscopy (yield = 85%) (Figure S1). The desired copolymers were then synthesized via free-radical polymerization using AIBN as a thermal initiator. The different feed ratios of ODA

and HEAm employed to prepare the various copolymers are listed in Table 1. Thus, ODA, HEAm, and AIBN (1 mol%, relative to the total monomer amount) were added to a pressure-resistant glass tube (ACE GLASS). Solvents of toluene and DMF were added to the glass tube at a volume ratio of 4:1 in a glove box filled with N_2 to give a total solute concentration of 0.2 M. The polymerization reaction was allowed to proceed at 60 °C for 12 h, after which time, the reaction tube was exposed to air, and the majority of the solvent evaporated under reduced pressure. When ODA:HEAm feed ratios of 7:3 and 6:4 were employed, the copolymers were initially precipitated using methanol prior to double precipitation using acetonitrile. The other copolymers were dissolved in chloroform and precipitated using acetonitrile as a poor solvent, and the reprecipitation process was repeated three times. The polymers were subsequently collected and dried at room temperature under reduced pressure. The monomer reactivity ratios, r_1 and r_2 (M_1 : HEAm and M_2 : ODA), were determined using a Fineman–Ross method (Figure S6)[38]

Polymer characterization

The synthesized compounds were characterized using ^{1}H and ^{13}C NMR spectroscopy on an ECA-500 JEOL spectrometer. All ^{1}H and ^{13}C NMR spectra were recorded in $CDCl_3$. The measurement temperature was 25 ˚C for ^{1}H and 45 ℃ for ^{13}C NMR. The monomer ratio in the copolymer was determined by integration of the methyl protons of ODA (~0.8 ppm) and the ethylene protons of HEAm (2.7–4.2 ppm) (Figure S2). The number-averaged molecular weights (M_n) and polydispersity indices (M_w/M_n) of the copolymers were measured using gel-permeation chromatography (GPC; Shodex GPC-101, Showa Denko K.K., Japan) at 40 ℃ with THF as the eluent and using polystyrene standards. The melting temperatures of the crystallized side chains (T_M) and the glass transition temperatures (T_g) of the copolymers were measured by differential scanning calorimetry (DSC, DSC8231, Rigaku Corp.) under a flow

of N_2 (50 mL min^{-1}) at a heating/cooling rate of 10 °C min^{-1} over a temperature range of −40–200 °C. For this purpose, the polymer powder (~5 mg) was added to the aluminum pan, and the third heating curve was used to obtain T_M and T_g.

Optical measurements

The Fourier transform infrared (FT-IR) spectra of the thin films were obtained using an FT-IR spectrometer (FT/IR 4200, Jasco Corp, Japan) with a resolution of 4 cm^{-1}.

X-ray scattering measurements

The X-ray-diffraction (XRD) and X-ray reflectivity (XRR) data were collected using a Smartlab X-ray diffractometer (Rigaku Corp.) equipped with a Cu Kα X-ray source (λ = 0.1542 nm) and a scintillation counter as a detector. The in-plane and out-of-plane XRD measurements of the thin films were carried out using a 1 cm^2 square silicon substrate coated with the desired polymer film. The out-of-plane XRD patterns were obtained using the $\theta/2\theta$ method with parallel-beam/parallel slit analyzer (PB) optics over a 2θ range of 1–40° with a step size of 0.02° (Figure S4a). The In-plane XRD patterns were obtained by the grazing incident mode at an incident angle of 0.20° using PB optics. The 2θ range was 1–25° and the step size was 0.008° (Figure S4b). The XRD pattern for the p(ODA50/HEAm50) powder was performed under the same conditions as those employed for the out-of-plane measurements (Figure S4a). Two-dimensional grazing-incidence X-ray diffraction (2D GI-XRD) measurements of the polymer thin films on the solid substrate were performed using small- and wide-angle X-ray scattering instruments (Nanoviewer, Rigaku Corp.) with a Cu Kα X-ray source (λ = 0.1542 nm) and a 2D detector (PILATUS 2M, Dectrics AG). The incidence angle was ~0.15° and the distance between the sample and the detector was 0.365 m. The X-ray was focused on an area with a diameter of 0.50 mm using three pinhole slits (diameters of 0.40, 0.20, and 0.45 mm).

A solid substrate coated with a polymer film was placed on the stage (ATS-C310-EM and ALV-300-HM, Chuo Precision Industrial Co., Ltd.) to control the tilt angle and height of the sample against the X-ray beam (Figure S4c).

Preparation of the thin films

The silicon and quartz substrates (Samco, Japan) were ultrasonically cleaned in acetone and then cleaned in isopropyl alcohol for 20 min. This cleaning procedure was repeated twice before the substrate surfaces were treated with UV–O_3 (PL16-110, SEN Lights Corp.) to prepare the hydrophilic substrate. To prepare the hydrophobic substrate, the hydrophilic substrate was immersed in a solution of trichloro(octyl)silane/chloroform (~1×10^{-5} M) for 1 d at room temperature. Thin films were prepared via a spin coating method (MA-A100, Mikasa), where a chloroform solution of the polymer was dropped onto a hydrophobic substrate. The spin-coated film was prepared by spinning at 1,000 rpm for 5 s and then at 2,500 rpm for 60 s. A polymer concentration of 5 wt% was used to prepare the films for the XRD and FT-IR measurements, while a concentration of 0.5 wt% was used to prepare the films for the XRR measurements. Each film prepared onto a hydrophobic Si substrate was annealed at the target temperature for a predetermined time, and subsequently, the substrate was immediately removed from the chamber and held at room temperature (20–25 °C). The annealing temperatures (T_g + ~10 °C) employed for the various copolymers were as follows: p(ODA40/60) = 100 °C, p(ODA50/HEAm50) = 115 °C, p(ODA60/HEAm40) = 108 °C, p(ODA70/HEAm) = 100 °C, and p(ODA90/HEAm10) = 95 °C.

RESULTS AND DISCUSSION

Syntheses and thermal properties of the p(ODA/HEAm) copolymers

Copolymers of ODA and HEAm were synthesized via free-radical copolymerization using AIBN as the thermal initiator (Figure S1,2, Scheme 1, Table 1). The ^{13}C NMR signals of the carbonyl carbon atoms, which are used to determine the tacticity of an acrylamide polymer,[40, 41] were observed as a broad peak (Figure S3), suggesting that the copolymers have no preferred stereoregularity and are atactic. A time–conversion study of the copolymerization process indicated that the HEAm monomer is converted more rapidly than the ODA monomer (Figure S5).[42] Using the Fineman–Ross method, the reactivity ratios of HEAm (M_1) and ODA (M_2) were determined to be $r_1 = 1.27$ and $r_2 = 0.63$ (Figure S6). These values are comparable to the calculated value ($r_1 = 1.23$ and $r_2 = 0.61$) using the Q and e values of HEAm[43] and ODA[44], thereby suggesting that the obtained copolymers are statistical copolymers.[45] We performed a classical batch copolymerization approach and the polymers were purified using a conventional reprecipitation approach and collected as white solids, and therefore, the polymer compositions listed in Table 1 correspond to an average value obtained based on all polymers present in the mixture. The thermal properties of the prepared copolymers were then investigated using DSC (Figure S7), wherein a strong exothermic peak can be observed at ~30 °C during the heating cycle. This peak was attributed to the melting of the crystalline octadecyl side chains (T_M) in the alkyl nanodomains,[15, 31] and it was found that, with the exception of p(ODA40/HEAm60), the T_M shifted to higher temperatures upon increasing the ODA content, due to the high crystallinity of the octadecyl side chains.[21] In addition, the baseline shift observed in the high-temperature region was attributed to the glass transition temperature (T_g). Decoupling of the side chain crystallization to the glass transition process strongly indicates that alkyl nanodomains formed in the bulk powders of the copolymers.[21] Furthermore, the T_g values of

p(HEAm) and p(ODA) are 117.6[46] and 83.2 °C,[31] and so the observed reduction in T_g upon increasing the ODA content (excluding p(ODA40/HEAm60)) indicates that the synthesized copolymers are statistical copolymers. It should be noted here that the reason for the exceptional thermal behavior (i.e., high T_M and T_g values) of the p(ODA40/HEAm60) copolymer is not currently understood. Overall, the DSC results indicate that the statistical copolymers do not possess a higher-order phase, such as a liquid-crystalline phase. The absence of the higher-order phase transition is consistent with the results of Ouchi et al.[35]

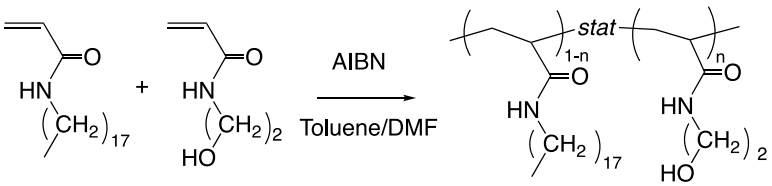

Scheme 1 Synthesis of the p(ODA/HEAm) statistical copolymers.

Table 1 Characterization of the p(ODA/HEAm) statistical copolymers

Copolymer	Molar feed ratio ODA: HEAm	Resulting molar ratio ODA: HEAm	*Mn*[b]	M_w/M_n[b]	T_g /°C[c]	T_M /°C[c]	*d* /nm
p(ODA10/HEAm90)[a]	10:90	-	-	-	-	-	-
p(ODA40/HEAm60)	30:70	36:64	7200	1.73	95.2	26.3	-
p(ODA50/HEAm50)	50:50	50:50	6600	2.15	104	22.7	3.7[d], 4.6[e]
p(ODA60/HEAm40)	60:40	64:36	16700	1.71	96.2	25.1	3.6[d], 4.4[e]
p(ODA70/HEAm30)	70:30	72:28	14200	1.79	92.1	29.5	3.3[d]
p(ODA90/HEAm10)	90:10	88:12	20700	1.72	82.4	30.8	-

a) A gel was formed and further characterization was not performed. b) Determined based on GPC measurements using polystyrene standards. c) Determined based on DSC measurements (Figure S7). d) Side-chain-mixed lamellae. e) Side-chain-segregated lamellae.

XRD measurements of the copolymer thin films

The copolymer thin films were prepared on a silicon substrate via spin coating and their structures were characterized using XRD measurements. None of the spin-coated films exhibited clear diffraction signals, suggesting that the initial films were amorphous (Figure 1, black lines). The broad scatterings observed in the XRD patterns of the thermally annealed (T_g + ~10 °C) films of p(ODA40/HEAm60) (q_{nd} ~1.4 nm^{-1}; Figure 1a) and p(ODA90/HEAm10) (q_{nd} ~1.8 nm^{-1}; Figure 1e) were attributed to diffraction from the alkyl nanodomains.[15, 31] Previously, our group reported that pODA exhibits a Bragg diffraction originating from its partially crystalized octadecyl side chains at ~4.0 nm^{-1}.[31] Thus, the diffraction signal observed at q_{cr} = 3.8 nm^{-1} (d = 1.6 nm) in the XRD pattern of the p(ODA90/HEAm10) film was attributed to the crystalized domains of octadecyl side chains.[31] The presence of alkyl nanodomains indicates that p(ODA40/HEAm60) and p(ODA90/HEAm10) are randomly oriented films,[15, 16] which is consistent with the DSC results. In addition, the diffraction patterns for p(ODA40/HEAm60) and p(ODA90/HEAm10) exhibited negligible changes upon increasing the annealing time to 24 h, and so it appeared that p(ODA40/HEAm60) was too hydrophilic and p(ODA90/HEAm10) was too hydrophobic to form a self-assembled structure via nanophase separation. Indeed, the two-dimensional grazing-incident XRD (2G-GIXRD) patterns of p(ODA40/HEAm60) and p(ODA90/HEAm10) were found to exhibit weak Debye-Scherrer rings (Figures S8a and S8b), thereby confirming the absence of a unidirectional orientation in these copolymer films.[15, 47]

On the other hand, the copolymers with HEAm contents ranging from 28 to 50% exhibit strong integer order peaks in their XRD patterns after thermal annealing (q_{lm}, Figures 1b–1d; green patterns), suggesting that the copolymer films form lamellar structures. Upon extending the annealing time to 24 h, the intensity of the Bragg peak increased, and the full width at half maximum (FWHM) values of the peaks decreased (Figures 1b–1d; red pattern). These results suggest that the lamellar uniformity increases with the annealing time, which is consistent with

previous results obtained from a dodecyl acrylamide/hydrophilic vinyl phosphoric acid copolymer.[34] Furthermore, the 2D-GIXRD images of the thermally annealed films of p(ODA50/HEAm50), p(ODA60/HEAm40), and p(ODA70/HEAm30) exhibited diffraction spots in the out-of-plane direction, where the q values were close to those of the first-order Bragg peaks in the corresponding 1D XRD patterns (Figure S9). These spot images demonstrate the formation of unidirectionally oriented lamellae in which the main chain forms a lamellar plane aligned parallel to the substrate plane, wherein the side chains are aligned perpendicularly to the main chains (inset in Figure 1) .[48] As revealed by the DSC measurements, the copolymers do not exhibit a liquid-crystalline phase (Figure S7). Furthermore, the lamellar periodicities of these films (d), which were calculated using the first Bragg peak for each film ($d = 2\pi/q$), were close to that obtained in the lamellar domains of aligned pODA fibers (Table 1).[36] It was therefore apparent that side-chain-mixed lamellae were formed in these copolymer films via segregation between the hydrophobic ODA side chains and the hydrophilic main-chain regions composed of amide and HEAm side chains.

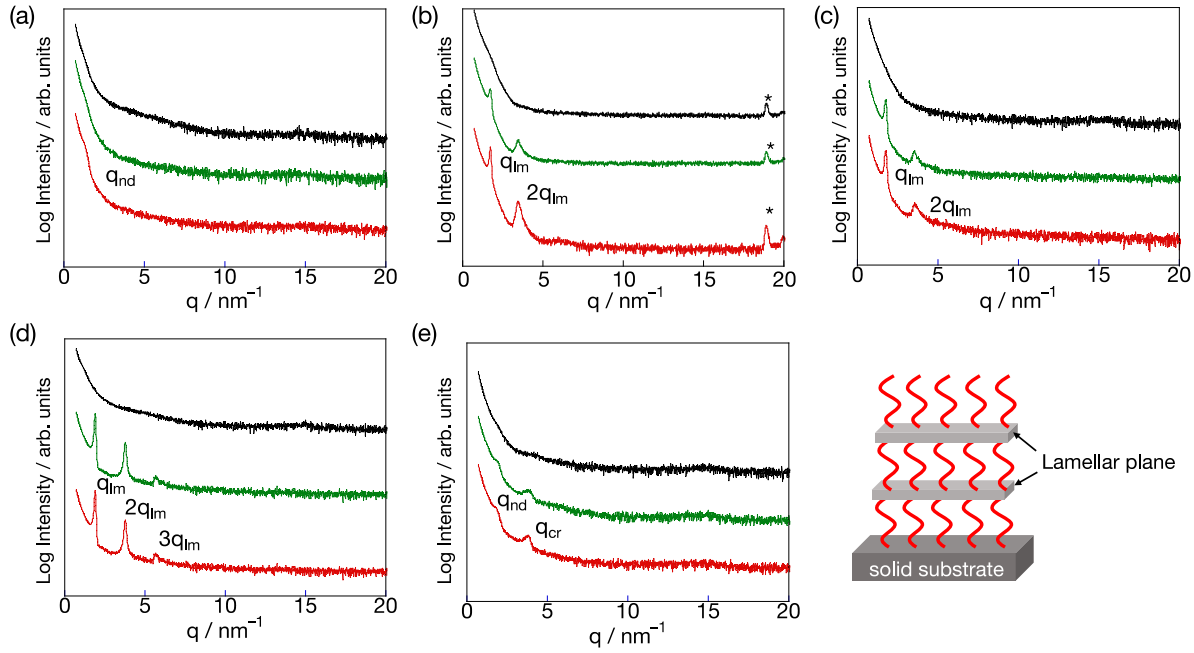

Figure 1 XRD patterns of the copolymers under different annealing times and conditions. (a) p(ODA40/HEAm60) (q_{nd} = 1.3 nm^{-1}), (b) p(ODA50/HEAm50) (q_{lm} = 1.7 and $2q_{lm}$ = 3.5 nm^{-1}). *Peak corresponding to the Si substrate), (c) p(ODA60/HEAm40) (q_{lm} = 1.8 and $2q_{lm}$ = 3.5 nm^{-1}), (d) p(ODA70/HEAm30) (q_{lm} = 1.9, $2q_{lm}$ = 3.8, and $3q_{lm}$ = 5.7 nm^{-1}), and (e) p(ODA90/HEAm10) (q_{nd} = 1.8 and q_{cr} = 3.9 nm^{-1}). For each sample, a pattern was recorded for the spin-coated film (black), the film following 90 min of thermal annealing *in vacuo* (green), and the film following 24 h of thermal annealing in air (red). Inset: Geometry of the lamellar structure toward the substrate.

Dependence of the lamellar structure on the annealing temperature

Subsequently, the effect of the annealing temperature on the lamellar film structure was determined, as presented in Figure 2. More specifically, in the XRD patterns recorded for the copolymer films annealed at different temperatures, it can be seen that the Bragg peaks of the

p(ODA50/HEAm50) film annealed at 120 °C broadened and shifted slightly to a lower q value. Further annealing resulted in a significant shift of the peaks to lower q values and sharpening of the peaks (Figures 2a and 3a). Indeed, the FWHM initially increased from 0.14 to 0.28 nm^{-1} upon increasing the temperature from 115 to 120 °C, whilst it subsequently decreased to 0.20 nm^{-1} at 160 °C (Figure 3a). Moreover, second-order Bragg diffraction peaks appeared in the patterns of the films annealed at 160 °C for 6 h (Figure S10), and the first-to-second-order peak position ratio (1:2) suggested that the copolymer transformed into another lamellar structure with a larger *d* value of 4.6 nm (Table 1). This large *d* value indicates that p(ODA50/HEAm50) formed side-chain-segregated lamellae upon annealing at 160 °C. Given that the thickness of a single layer of side-chain-segregated lamellae is equal to the sum of two interdigitated octadecyl side chains plus the length of the hydroxyethyl side chain (see Figure 7b), it is higher than the corresponding values observed for the side-chain-mixed lamellae. It was therefore considered that the lamellae formed upon annealing at T_g + ~10 °C (Figures 1b–1d) are side-chain-mixed lamellae, wherein the thickness of a single layer (*d*) is equal to the sum of two interdigitated octadecyl side chain lengths (Figure 7a). Additionally, the 2D-GIXRD image obtained for the p(ODA50/HEAm50) film annealed at 160 °C for 1.5 h exhibited spot-like peaks at q = 1.2 nm^{-1} (side-chain-segregated lamellae) and at q = 1.6 nm^{-1} (side-chain-mixed lamellae) (Figure S11a). The simultaneous appearance of these two peaks suggests that upon elevating the annealing temperature, the side-chain-mixed lamellae transformed into side-chain-segregated lamellae. As shown in the XRD pattern of the p(ODA70/HEAm30) polymer (Figure 2c), increasing the temperature resulted in disorder of the lamellar structure, wherein the peak intensity gradually decreased and the peak broadened. On the other hand, if an increase in temperature were to enhance the lamellar uniformity, the Bragg peak positions would remain almost unchanged, and the peaks would become sharper and more intense; no such observations were made. The simultaneous appearance of diffraction from side-chain-

segregated and side-chain-mixed lamellae in the 2D-GIXRD image indicates that not all the mixed lamellae transit to segregated lamellae. Deconvolution of the first Bragg peak at the 1D XRD pattern indicates that 89% of the mixed lamellae transited to segregated lamellae after annealing at 160 ˚C (Figure S10c).

It was also found that in the context of the XRD patterns, increasing the annealing temperature of the p(ODA60/HEAm40) film resulted in similar trends to those observed for the p(ODA50/HEAm50) film. More specifically, a significant shift of the Bragg diffraction peaks to lower q values was observed as the annealing temperature increased (Figures 2b and 3b), whilst the 2D-GIXRD image for the film annealed at 160 °C for 1.5 h exhibited spot-like peaks at q = 1.2 nm^{-1} (side-chain-segregated lamellae) and at q =1.7 nm^{-1} (side-chain-mixed lamellae) (Figure S11b). Conversely, the FWHM gradually increased upon increasing the temperature (Figure 3b), and the observation of broad diffraction peaks suggests that the uniformity of the side-chain-segregated lamellae of p(ODA60/HEAm40) was low. Upon increasing the annealing temperature from 120 to 140 °C significant changes were found for the q values of p(ODA50/HEAm50) and p(ODA60/HEAm40), suggesting that an order–order transition from the side-chain-mixed lamellae to the side-chain-segregated lamellae began in this temperature range. In addition, upon increasing the annealing temperature from 100 °C (T_g + 10 °C) to 120 °C, the Bragg diffraction peaks in the p(ODA70/HEAm30) pattern broadened significantly, becoming shoulder-like upon annealing at temperatures >140 °C (Figures 2c and 3c). The presence of such shoulder-like diffraction signals indicate that the structure of the film becomes random and forms alkyl nanodomains. The broad peak that appeared at ~3.7 nm^{-1} was attributed to the crystallized domains of ODA, and so it appeared that annealing p(ODA70/HEAm30) at higher temperatures resulted in the formation of a randomly oriented film with crystallized ODA nanodomains, similar to those observed in p(ODA90/HEAm10). Indeed, the 2D-GIXRD pattern of the film annealed at 160 °C only exhibited a Debye–Scherrer

ring at q = 1.8 nm^{-1}, which was attributed to diffraction from the alkyl nanodomains (Figure S11c). Thus, p(ODA70/HEAm30) transforms from an ordered side-chain mixed lamellar structure to a disordered random structure at approximately 140 °C.

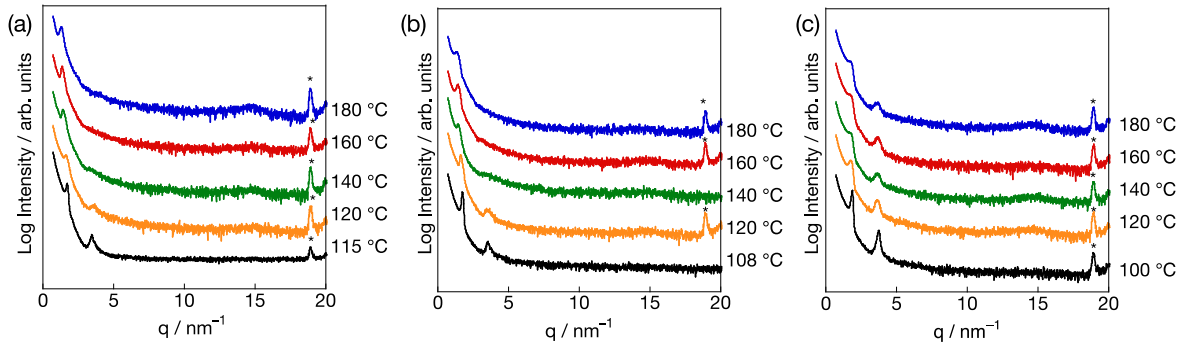

Figure 2. XRD patterns of the copolymer lamellar structures formed at different annealing temperatures. (a) p(ODA50/HEAm50), (b) p(ODA60/HEAm40), and (c) p(ODA70/HEAm30). *The peak corresponds to diffraction from the Si substrate.

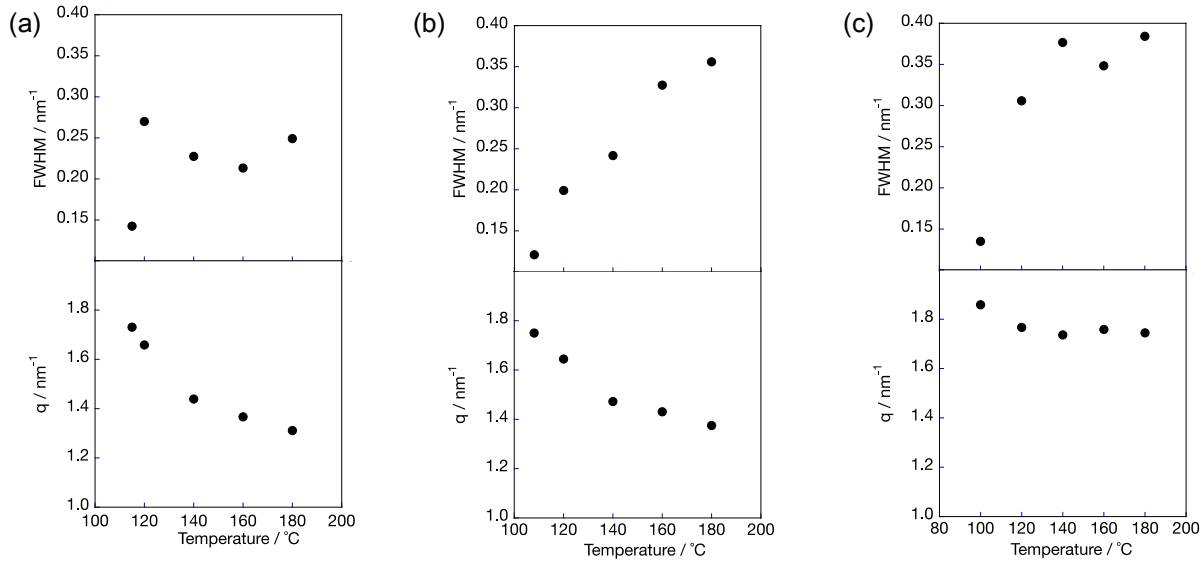

Figure 3 FWHM (top) and q values (bottom) of the first-order peaks observed at different annealing temperatures. (a) p(ODA50/HEAm50), (b) p(ODA60/HEAm40), and (c) p(ODA70/HEAm30). The FWHM and q values were obtained by Gaussian fitting of the first-order peaks using Multi-peak fitting in Igor Pro9 (Wavemetrics).

In-plane XRD study of the lamellar films

In-plane XRD measurements were conducted to study the packing of the octadecyl side chains in the lamellar films. Figure 4 shows the in-plane XRD patterns of the copolymer lamellar films prepared from p(ODA70/HEAm30), p(ODA60/HEAm40), and p(ODA50/HEAm50), wherein the peak observed at ~15 nm^{-1} (q_{hex}) originates from hexagonally packed crystals generated from the alkyl chains.[49] It has been reported that the q_{hex} position shifts toward higher q values and results in a narrower diffraction with an increase in crystallinity.[49] Consequently, the diffraction peak at ~15 nm^{-1} was fit with a single Gaussian peak to obtain q_{hex} and the FWHM (Figure S12). As outlined in Table 2, the q_{hex} values of the lamellar films remained at almost identical positions regardless of the ODA content, whereas the FWHM decreased with an increase in the ODA content. The FWHM of the p(ODA50/HEAm50) specimen annealed at 160 °C exhibited the highest value, indicating the low crystallinity of the ODA side chains. It should be noted here that in a statistical copolymer, it is challenging to orient the octadecyl side chains in a single direction, ultimately resulting in significant strain on the main chain and steric hindrance between the octadecyl side chains. As a result, the ODA side chains are less crystalline in the segregated lamellar films.

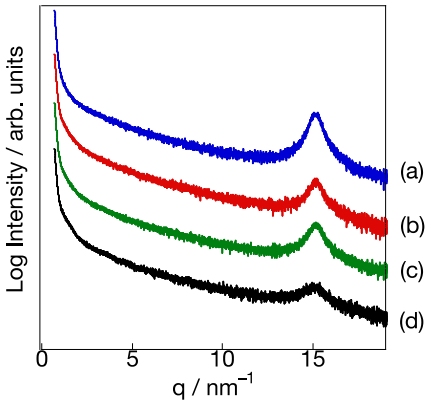

Figure 4 In-plane XRD patterns for the lamellar films: (a) p(ODA70/HEAm30) annealed at 110 °C for 24 h, (b) p(ODA60/HEAm40) annealed at 108 °C for 24 h, (c) p(ODA50/HEAm50) annealed at 115 °C for 24 h, and (d) p(ODA50/HEAm50) annealed at 160 °C for 6 h.

Table 2 FWHM and q_{hex} values for the lamellar films

Copolymer	q_{hex} / nm^{-1}	FWHM / nm^{-1}
p(ODA50/HEAm50) annealed at 160 °C	15.06	1.30
p(ODA50/HEAm50) annealed at 115 °C	15.13	1.04
p(ODA60/HEAm40) annealed at 108 °C	15.14	0.97
p(ODA70/HEAm30) annealed at 110 °C	15.13	0.92

The q_{hex} and FWHM values were obtained by Gaussian fitting of the first-order peak using multi-peak fitting in Igor Pro9 (Wavemetrics).

FT-IR study of the mixed and segregated lamellar films

FT-IR spectroscopy was subsequently employed to confirm the differences in the octadecyl side chain packing for the two lamellar structures. Previously, it has been reported that the CH_2 stretching absorption is dependent on the hydrocarbon conformation. More specifically, when the hydrocarbon chain is in an all-*trans* zigzag conformation, symmetric (ν_s) and asymmetric (ν_a) vibrational modes appear at 2848 ± 1 and 2918 ± 1 cm^{-1}, respectively. In addition, these peaks shift to higher wavenumbers with an increase in the prevalence of the gauche

conformation.[50, 51] In the current study, it was found that the peak positions of ν_s and ν_a for the mixed and segregated lamellar films were comparable, whereas the absorption peak observed for the segregated lamellar film was broad with a shoulder at a higher wavenumber (Figure 5). For example, deconvolution of the ν_a peaks appeared ~2918 cm^{-1} indicates that the content of the *gauche* conformation in the octadecyl side chains of the segregated lamellar film is 1.2 times higher than that of the mixed lamellar film (Figure S13). Indeed, the in-plane XRD and FT-IR results show that octadecyl side chains in the mixed lamellae are mostly all-*trans* and crystalline, whereas the segregated lamellae contain a higher prevalence of *gauche* structures and are less crystalline. It has been reported that an increase in the *gauche* content results in a decrease in the lamellar periodicity in a mixed lamellar structure.[21] However, the opposite was observed for the current systems, thereby indicating that the structural change is not related to changes in the side chain crystallinity and/or the degree of interdigitation, but to the transition from mixed to segregated lamellae.

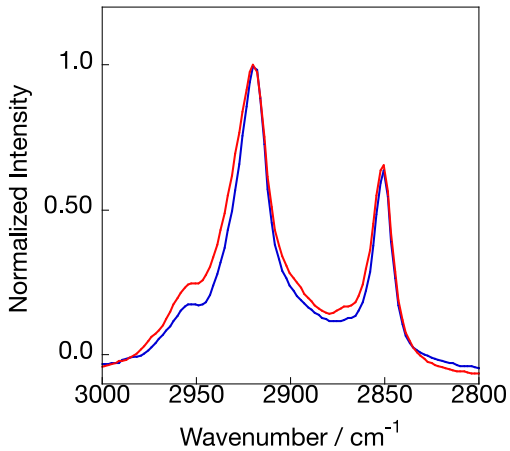

Figure 5 FT-IR spectra of the p(ODA50/HEAm50) film annealed at 115 °C for 24 h (blue) and at 160 °C for 6 h (red).

XRR study of the p(ODA50/HEA50) film

The two lamellar structures were further characterized using XRR analysis. As shown in Figures 6a and 6c, the XRR patterns contain low-angle fringes for the films annealed at 115 and 160 °C, with a Bragg diffraction at q = 1.6 nm^{-1} for the film annealed at 115 °C and at q = 1.3 nm^{-1} for the film annealed at 160 °C. These q values are comparable to the 1st order Bragg diffractions observed in the XRD patterns (Figures 1d and 2a). Subsequently, the obtained XRR patterns were fit using a two-box model with alternating hydrophobic and hydrophilic layers (Figures 6a and 6b),[52, 53] and it was found that the XRR patterns could be explained by the periodic scattering length density (SLD) profiles, thereby supporting the formation of a lamellar structure. The thicknesses of the hydrophilic regions obtained by the fitting for the side-chain-segregated and mixed lamellae were similar, i.e., 5.9 Å for the side-chain-segregated lamellae and 5.4 Å for the side-chain-mixed lamellae. The length of HEAm was calculated to be 5.4 Å in the stretched conformation (Figure S14), which indicates that the HEAm moieties are interdigitated with one another in the segregated lamellae. On the other hand, the hydrophobic layer formed by the alkyl chains was found to be 8 Å longer in the segregated structure (42 Å) than in the mixed structure (34 Å) (Figures 7a and 7b). This was attributed to the fact that in the side-chain-segregated lamellar structure, the hydrophobic layer is formed entirely by the octadecyl side chains, whereas in the side-chain-mixed lamellar structure, some of the alkyl chains overlap with the hydrophilic layer, resulting in a thinner hydrophobic layer. The densities of the hydrophilic (ρ_{philic}) and hydrophobic (ρ_{phobic}) layers obtained from the fitting results indicated that both densities were larger in the mixed system (ρ_{philic} = 0.40 g cm^{-3}, ρ_{phobic} = 0.30 g cm^{-3}) than in the segregated lamellar film (ρ_{philic} = 0.24 g cm^{-3}, ρ_{phobic} = 0.28 g cm^{-3}) due to the well-packed structure of the former. Moreover, the difference between ρ_{philic} and ρ_{phobic} in each lamella reflects the difference in their layer structure. In the mixed lamellar film, the hydrophobic layer is formed only by ODA side

chains, whereas the hydrophilic layer is composed of the amide group of ODA and HEAm. Thus, ρ_{philic} is larger than ρ_{phobi}. On the other hand, the segregated lamella is constructed from partially crystallized ODA side chains as a hydrophobic layer and amorphous HEAm side chains as a hydrophilic layer, which resulted in $\rho_{philic} < \rho_{phobic}$. These results supported the previously discussed in-plane and FT-IR measurements. The XRR results therefore confirm that annealing at 115 °C produces a mixed lamellar structure, while annealing at 160 °C generates a segregated lamellar structure.

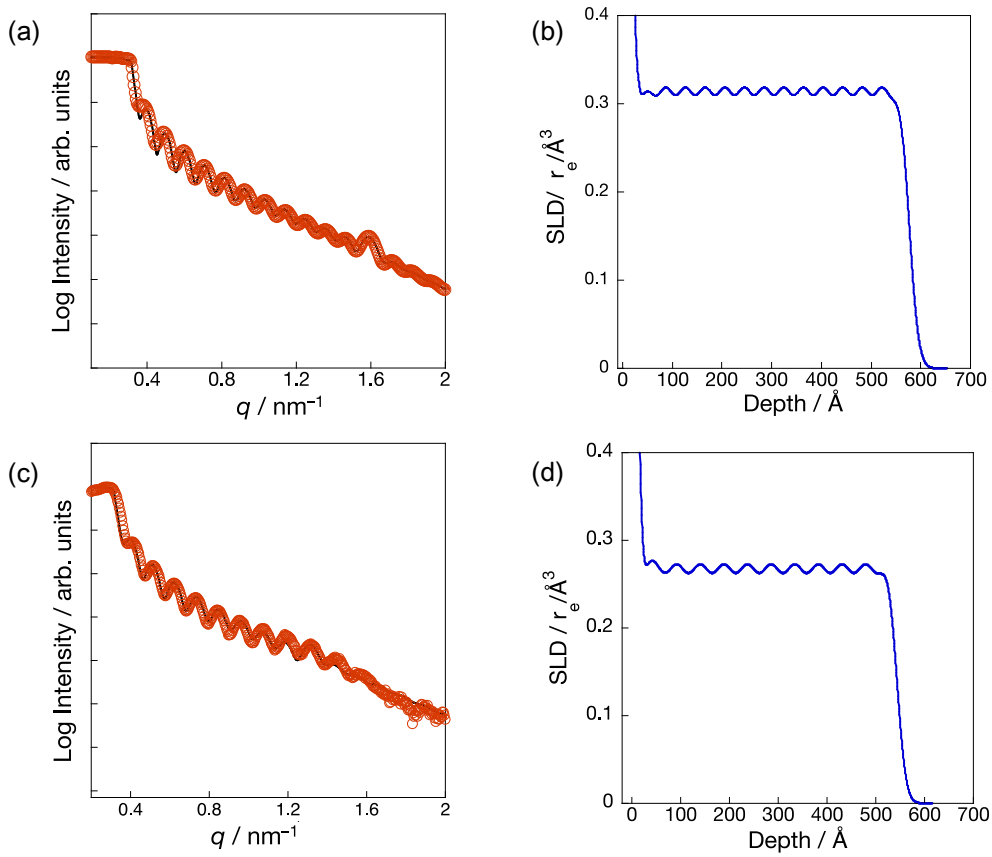

Figure 6. XRR patterns (a,c) and SLD profiles (b,d) of the p(ODA50/HEAm50) films annealed at 115 ℃ for 1.5 h (a, b) and at 160 ℃ for 1.5 h (c, d). The XRR patterns and fitting results are shown as red circles and black lines, respectively in (a, c).

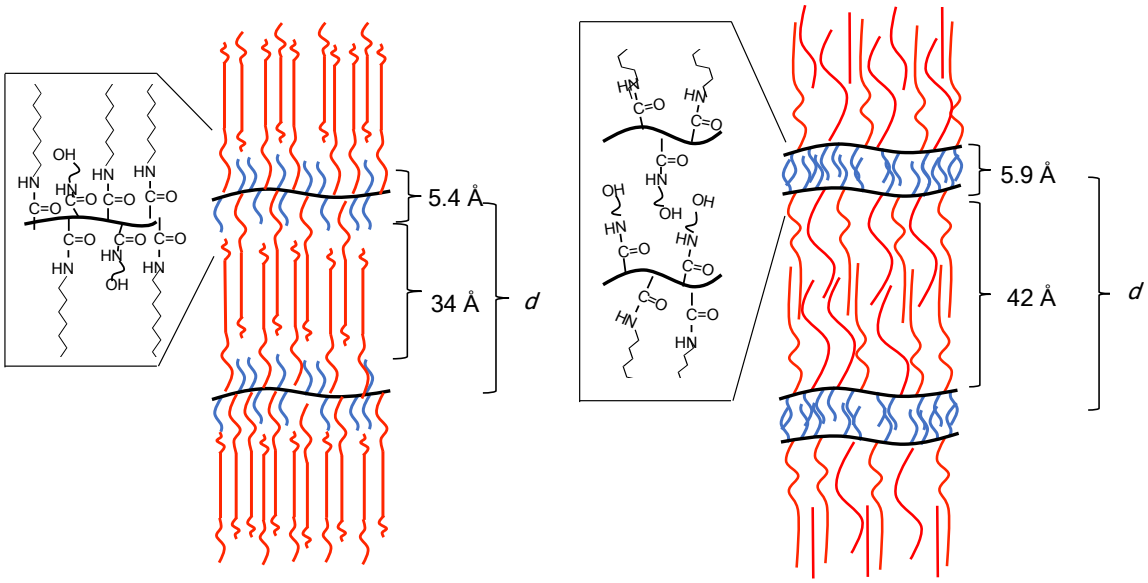

Figure 7. Two box model used in fitting p(ODA50/HEAm50) film annealed at (a)115°C for 1.5 h (side-chain-mixed lamellae) and (b) 160°C for 1.5 h (side-chain-segregated lamellae). The hydrophobic and hydrophilic layers in the 2-box model are indicated by red and blue boxes, respectively. The crystallized ODA regions are expressed as dark red box. Black, red, and blue lines represent –(CH_2-CH)- main chain, octadecyl + amide, and hydroxyethyl + amide groups respectively.

Proposed mechanism for the influence of temperature on the lamellar structure

The dependence of the lamellar structure on the annealing temperature and the copolymer composition can be related to the competition between the strain generated by the orientation of the side chains and the miscibility of the comonomers. To form side-chain-segregated lamellae, identical side chains (ODA or HEAm) must be aligned in the same direction relative to the main chain (Figure 7b). This orientation creates significant strain in these statistical

copolymers. For example, in a continuous ODA-ODA sequence, sizeable steric hindrance between the octadecyl side chains must be overcome to align the long octadecyl side chains in the same direction, which generates considerable strain on the main chain. As revealed by the in-plane XRD and FT-IR measurements discussed above, these strains resulted in low orientation and crystallinity degrees for the ODA side chains in the prepared copolymers, wherein the segmental mobility of the polymer chains at temperatures slightly above T_g was not sufficient to exceed the strain energy. As a result, annealing at T_g + 10 °C led to the formation of side-chain-mixed lamellae, wherein the HEAm comonomers "mix" with the ODA comonomers and form a hydrophilic "main chain" containing amide groups (Figure 7a). The hydrophilic HEAm side chains increase the hydrophilicity around the main chain, ultimately inducing segregation of the octadecyl side chains from the main chain.

However, considering the miscibility of the comonomers, phase separation between the hydrophobic octadecyl and hydrophilic hydroxyethyl side chains is preferred. Therefore, when the thermal energy becomes sufficiently high to overcome the steric hindrance and strain, segregation between the hydrophilic and hydrophobic comonomers dominates the self-assembly process to form side-chain-segregated lamellae. As a result, p(ODA50/HEAm50) and p(ODA60/HEAm40) transformed from side-chain-mixed to side-chain-segregated lamellae at ~140 °C. In addition, the XRD pattern of p(ODA60/HRAm40) broadened upon annealing at 180 °C, suggesting that the lamellar structure became disordered owing to the violent motion of the polymer chains. Furthermore, the segregation force between the comonomers in p(ODA70/HEAm30) was weak owing to the low content of hydrophilic HEAm groups, and as a result, this polymer converted directly from a side-chain-mixed lamellar structure to a disordered state.

Thermo-reversibility study of the lamellar film

A thermo-reversibility study was carried out for the transition between the mixed lamellae and side-chain-segregated lamellae. For this purpose, a spin-coated film of p(ODA50/HEAm50) on a Si substrate was annealed at 115 °C for 1.5 h and its XRD pattern was recorded to confirm the formation of a mixed lamellar structure (Figures 8a black pattern). The mixed lamellar film was then annealed at 160 °C for 3 h (referred to as the re-annealed film), and it was found that the XRD pattern for the re-annealed film exhibited a similar pattern to that directly annealed at 160 °C (Figure 8a green pattern); importantly, this result suggests a transition from a mixed lamellar structure to a segregated lamellar structure (Figure 8a). To discuss the transition from the segregated to mixed lamellae, spin coated film of p(ODA50/HEAm50) on a Si substrate was directly annealed at 160 ˚C for 3 h (Figure 8b green pattern), then re-annealing at 115 ˚C. The film re-annealed at 115 °C showed negligible changes even after allowing the annealing process to continue for 9 h, which suggests that the transition from segregated lamellae to mixed lamellae did not occur. As described above in the context of the self-assembly mechanism, the formation of segregated lamellae requires a significant energy input to overcome the steric hindrance, and a temperature of 115 °C is clearly not sufficient for this purpose.

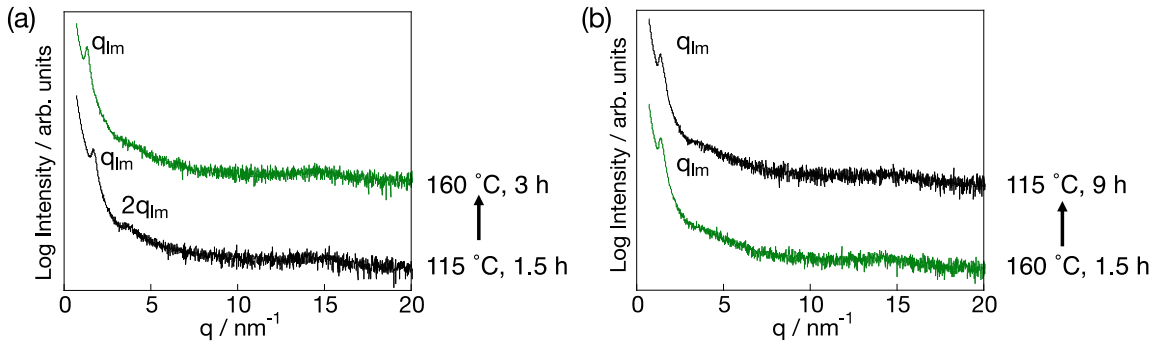

Figure 8 XRD patterns of the p(ODA50/HEAm50) thin film: (a) Initially annealed at 115 °C for 1.5 h (black), then re-annealed at 160 °C for 3 h (green); (b) initially annealed at 160 °C for 3 h (green), then re-annealed at 115 °C for 9 h (black).

Bulk powder study

Finally, the effect of thermal annealing on the structure of the p(ODA50/HEAm50) bulk powder was examined. As shown in Figure S15, the powder XRD pattern of the p(ODA50/HEAm50) film that was recorded following annealing at 115 °C for 24 h exhibited broad diffractions arising from the alkyl nanodomains (q_{nd} = 1.6 nm^{-1})[15] and the crystallized ODA side chains (q_{cr} = 3.6, q_{hex} = 15 nm^{-1}).[31] In contrast, no diffractions originating from the highly oriented lamellar structure were observed. This result is similar to that reported by Ouchi et al., i.e., the bulk powder of the random p(OD50/HEAm50) copolymer does not form an ordered structure.[35] Our results therefore indicate that the formation of lamellar structures in p(ODA/HEAm) is specific to thin films. At present, we believe that a hydrophobic air/polymer interface with a large free volume is the key to the formation of the observed lamellae.

CONCLUSIONS

The formation of uniform lamellar structures is known to take place in statistical copolymers via segregation between the main chain and the side chains or comonomers. It was found that in such systems, the generated lamellar morphologies are influenced by the annealing temperature employed and the ratio of the two comonomers (i.e., *N*-octadecyl acrylamide (ODA) and hydroxyethyl acrylamide (HEAm)). More specifically, copolymers with HEAm contents between 28 and 50% formed side-chain-mixed lamellae upon thermal annealing at T_g + 10 °C. Moreover, the p(ODA50/HEAm50) and p(ODA60/HEAm40) copolymers were found to undergo an order–order transition from a side-chain-mixed lamellar structure to a side-chain-segregated lamellar structure at ~140 °C. Owing to the weak segregation forces between the comonomers, other copolymer compositions were not observed to form self-assembled structures. It was therefore proposed that the generation of such self-assembled structures is dependent on the segregation forces and strains induced during the self-assembly process. It is

expected that the present results will aid in the preparation of new phase diagrams for self-assembled structures in statistical copolymers. The influences of the hydrophilic groups and side-chain structures of the comonomers on the lamellar formation process are currently being investigated in our laboratory, and the results will be presented in due course.

ASSOCIATED CONTENT

Supporting Information

The Supporting Information is available free of charge

Experimental details, ^{1}H ^{13}C NMR spectra of ODA and copolymers, time-conversion curves, Fineman-Ross plot, DSC spectra, 2D-XRD images of the copolymers and fitting results for the spectra.

AUTHOR CONTRIBUTIONS

M. K. and N. S. carried out all the synthesis of the copolymers and characterization of the film. M. K. wrote the first draft of the paper. S. N. analyzed the XRD and XRR results, M. O. and S. N. carried out XRR measurements. J. M. directed the whole project and wrote the final version of the manuscript.

AUTHOR INFORMATION

Corresponding Author

Jun Matsui

Faculty of Science, Yamagata University, 1-4-12 Kojirakawa-machi, Yamagata 990-8560, Japan

ORCID 0000-0003-4767-4507

*E-mail: jun_m@sci.kj.yamagata-u.ac.jp

Conflict of interest

There are no potential conflicts of interest to declare

ACKNOWLEDGMENTS

This work was supported by KAKENHI grant 18H02026 from the Japan Society for the Promotion of Science (JSPS), the JST, CREST grant number JPMJCR21B5, 2021 Yamagata University – Center of Excellence (Collaboration) (YU-COE(C)) program, the "Yamagata University Carbon Neutral Research Center (YUCaN)," THE TOYO SUISAN FOUNDATION, and the Research Program "Dynamic Alliance for Open Innovation Bridging Human, Environment and Materials" within the "Network Joint Research Center for Materials and Devices."

REFERENCE

1. M. W. Matsen and F. S. Bates, *Macromolecules*, 1996, **29**, 1091.
2. L. Leibler, *Macromolecules*, 1980, **13**, 1602.
3. F. S. Bates and G. H. Fredrickson, *Physics Today*, 1999, **52**, 32.
4. H. W. Ian, *The Physics of Block Copolymers*, Oxford Science, New York, 1999.
5. S. Sakurai, T. Momii, K. Taie, M. Shibayama, S. Nomura and T. Hashimoto, *Macromolecules*, 1993, **26**, 485.
6. J. K. Kim, S. Y. Yang, Y. Lee and Y. Kim, *Progress in Polymer Science*, 2010, **35**, 1325.
7. F. S. Bates and G. H. Fredrickson, *Annual Review of Physical Chemistry*, 1990, **41**, 525.
8. C. Maier and T. Calafut, in *Polypropylene*, eds. C. Maier and T. Calafut, William Andrew Publishing, Norwich, NY, 1998, pp. 11.
9. S. Dailey, W. J. Feast, R. J. Peace, I. C. Sage, S. Till and E. L. Wood, *Journal of Materials Chemistry*, 2001, **11**, 2238.
10. F. Dumur, Y. Guillaneuf, A. Guerlin, G. Wantz, D. Bertin, F. Miomandre, G. Clavier, D. Gigmes and C. R. Mayer, *Macromol Chem Phys*, 2011, **212**, 1616.
11. C.-A. Dai, B. J. Dair, K. H. Dai, C. K. Ober, E. J. Kramer, C.-Y. Hui and L. W. Jelinski, *Phys Rev Lett*, 1994, **73**, 2472.
12. P. Mansky, Y. Liu, E. Huang, T. P. Russell and C. Hawker, *Science*, 1997, **275**, 1458.
13. L. Li, K. Raghupathi, C. Song, P. Prasad and S. Thayumanavan, *Chemical Communications*, 2014, **50**, 13417.
14. M. Beiner, K. Schröter, E. Hempel, S. Reissig and E. Donth, *Macromolecules*, 1999, **32**, 6278.
15. M. Beiner and H. Huth, *Nat Mater*, 2003, **2**, 595.

16. S. Hiller, O. Pascui, H. Budde, O. Kabisch, D. Reichert and M. Beiner, *New Journal of Physics*, 2004, **6**, 10.

17. S. Pankaj and M. Beiner, *The Journal of Physical Chemistry B*, 2010, **114**, 15459.

18. M. Beiner, *Macromol Rapid Comm*, 2001, **22**, 869.

19. M. Beiner, O. Kabisch, S. Reichl and H. Huth, *Journal of Non-Crystalline Solids*, 2002, **307–310**, 658.

20. E. Hempel, H. Huth and M. Beiner, *Thermochim Acta*, 2003, **403**, 105.

21. E. Hempel, H. Budde, S. Höring and M. Beiner, *Journal of Non-Crystalline Solids*, 2006, **352**, 5013.

22. V. Danke, G. Gupta, S. Reimann, W. H. Binder and M. Beiner, *Eur Polym J*, 2018, **103**, 116.

23. T. Ikami, Y. Kimura, M. Takenaka, M. Ouchi and T. Terashima, *Polymer Chemistry*, 2021.

24. G. Hattori, M. Takenaka, M. Sawamoto and T. Terashima, *J Am Chem Soc*, 2018, **140**, 8376.

25. E. Hempel, H. Budde, S. Höring and M. Beiner, in *Progress in Understanding of Polymer Crystallization*, eds. G. Reiter and G. R. Strobl, Springer Berlin Heidelberg, Berlin, Heidelberg, 2007, pp. 201.

26. C. B. Mcardle, *Side Chain Liquid Crystal Polymers*, Springer Dordrecht, 1989.

27. N. A. Platé and V. P. Shibaev, *Comb-Shaped Polymers and Liquid Crystals*, Springer US, New York, 1987.

28. K. Matsunaga, W. Kukai, M. Ishizaki, M. Kurihara, S. Yamamoto, M. Mitsuishi, H. Yabu, S. Nagano and J. Matsui, *Macromolecules*, 2020, **53**, 9601.

29. S. Ito, K. Matsunaga and J. Matsui, *Molecular Crystals and Liquid Crystals*, 2019, **685**, 7.

30. K. Ebata, T. Togashi, S. Yamamoto, M. Mitsuishi and J. Matsui, *J Electrochem Soc*, 2019, **166**, B3218.

31. K. Ebata, Y. Hashimoto, S. Yamamoto, M. Mitsuishi, S. Nagano and J. Matsui, *Macromolecules*, 2019, **52**, 9773.

32. K. Ebata, Y. Hashimoto, K. Ebara, M. Tsukamoto, S. Yamamoto, M. Mitsuishi, S. Nagano and J. Matsui, *Polymer Chemistry*, 2019, **10**, 835.

33. Y. Hashimoto, T. Sato, R. Goto, Y. Nagao, M. Mitsuishi, S. Nagano and J. Matsui, *RSC Adv.*, 2017, **7**, 6631.

34. A. Niinuma, M. Tsukamoto and J. Matsui, *Langmuir*, 2021, **37**, 5393.

35. Y. Kametani, F. Tournilhac, M. Sawamoto and M. Ouchi, *Angewandte Chemie-International Edition*, 2020, **59**, 5193.

36. H. W. S. Hsieh, B. Post and H. Morawetz, *Journal of Polymer Science: Polymer Physics Edition*, 1976, **14**, 1241.

37. T. Ikami, Y. Watanabe, H. Ogawa, M. Takenaka, N. L. Yamada, M. Ouchi, H. Aoki and T. Terashima, *ACS Macro Letters*, 2021, **10**, 1524.

38. R. J. Young and P. A. Lovell, *Introduction to Polymers*, Third Edition edn., Tailor & Francis, Florida, 2011.

39. T. Nishida, K. Satoh and M. Kamigaito, *Molecules*, 2020, **25**.

40. T. Hirano, T. Kamikubo, Y. Okumura, Y. Bando, R. Yamaoka, T. Mori and K. Ute, *J. Polym. Sci. A Polym.*, 2009, **47**, 2539.

41. M. Kobayashi, S. Okuyama, T. Ishizone and S. Nakahama, *Macromolecules*, 1999, **32**, 6466.

42. D. Oh, Y. Furuya and M. Ouchi, *Macromolecules*, 2019, **52**, 8577.

43. S. Ida, D. Nishisako, A. Fujiseki and S. Kanaoka, *Soft Matter*, 2021, **17**, 6063.

44. J. Brandrup, E. H. Immergut and E. A. Grulke, eds., *Polymer Handbook*, 4 edn., Wiley, 2003.

45. A. D. Jenkins and K. L. Loening, in *Comprehensive Polymer Science and Supplements*, eds. G. Allen and J. C. Bevington, Pergamon, Amsterdam, 1989, pp. 13.

46. A. Narumi, Y. Chen, M. Sone, K. Fuchise, R. Sakai, T. Satoh, Q. Duan, S. Kawaguchi and T. Kakuchi, *Macromol Chem Phys*, 2009, **210**, 349.

47. B. Lee, I. Park, J. Yoon, S. Park, J. Kim, K. W. Kim, T. Chang and M. Ree, *Macromolecules*, 2005, **38**, 4311.

48. S. Nagano, *Langmuir*, 2019, **35**, 5673.

49. M. Mierzwa, G. Floudas, P. Štepánek and G. Wegner, *Physical Review B*, 2000, **62**, 14012.

50. Z. Zhang, A. L. Verma, M. Yoneyama, K. Nakashima, K. Iriyama and Y. Ozaki, *Langmuir*, 1997, **13**, 4422.

51. J. Umemura, D. G. Cameron and H. H. Mantsch, *Biochim Biophys Acta*, 1980, **602**, 32.

52. M. Björck and G. Andersson, *Journal of Applied Crystallography*, 2007, **40**, 1174.

53. S. Yamamoto, N. Nishina, J. Matsui, T. Miyashita and M. Mitsuishi, *Langmuir*, 2018, **34**, 10491.